DOI: 10.67692/IODT.26.7900

Integrated Oncology Diagnostics & Treatment
Volume 1, Issue 2, 2026 | Pages 108-124 | ISSN: 2979-5575
Published by Pinnacle Academic Publishing, United Kingdom

REVIEW ARTICLE

Real-Time Intrafraction Motion Management in Magnetic Resonance Imaging-Guided Adaptive Radiotherapy and Its Impact on Treatment Precision

Manar Salah[1], Ahmed Shawky[1], Eman Gamal[1], Eman Helmy[1], Alaa Shawkat[1], Rasha Adel Abdelmoneum[1]

[1] *Clinical Oncology Department, Faculty of Medicine, Menoufia University, Egypt*

Abstract

Background and Purpose: Intrafraction motion remains a principal source of geometric uncertainty in external beam radiotherapy. Magnetic resonance imaging-guided adaptive radiotherapy (MRgART) uses continuous soft-tissue visualization throughout beam delivery to directly manage this uncertainty. This review critically evaluated the current state of real-time intrafraction motion management in MRgART, with emphasis on technological mechanisms, site-specific motion characteristics, clinical strategies, and the available evidence base.

Materials and Methods: A structured narrative review of peer-reviewed literature, prospective registries, and international consensus documents published through March 2026 was conducted. PubMed/MEDLINE was searched using terms encompassing MR-Linac platforms, intrafraction motion, real-time gating, and adaptive radiotherapy. A total of 47 references meeting pre-specified inclusion criteria were synthesized.

Results: Two commercial MR-Linac platforms dominated clinical practice: the 1.5 T system (>150 installed units) and the 0.35 T system (~55–65 operational units following corporate restructuring in 2024). Real-time beam gating reduced mean two-dimensional target displacement from 8.3 ± 4.3 mm (ungated) to 1.6 ± 0.6 mm (gated). A phase III randomized trial demonstrated that magnetic resonance imaging-guided stereotactic body radiotherapy for prostate cancer halved two-year late genitourinary toxicity compared with computed tomography-guided treatment (27% vs 51%; p = 0.004). A multi-institutional phase II trial established that ablative pancreatic stereotactic body radiotherapy (50 Gy in 5 fractions) was deliverable with near-zero severe gastrointestinal toxicity and a median overall survival of 22.8 months from diagnosis. Artificial intelligence approaches achieved sub-millimeter target localization at inference times of 8–36 milliseconds.

Conclusions: Magnetic resonance imaging-guided intrafraction motion management was selectively transformative, enabling treatments previously limited by geometric uncertainty. Expansion of randomized evidence beyond prostate cancer, resolution of workflow efficiency constraints, and clinical deployment of artificial intelligence-assisted real-time tracking represented the field's foremost priorities.

Keywords: Magnetic Resonance-Guided Adaptive Radiotherapy; Intrafraction Motion Management; Real-Time Tumor Tracking; Respiratory Gating; Treatment Precision.

Corresponding Author:
Manar Salah, Clinical Oncology Department, Faculty of Medicine, Menoufia University, Egypt.
E-mail: *mannar.ali@med.menofia.edu.eg*
Address: Yassin Abdel Ghaffar street, Shebin Elkom, postal code 32511, Egypt

Received 7 August 2026
Revised 12 September 2026
Accepted 1 October 2026
Published 1 November 2026

DOI: 10.67692/IODT.26.7900

How to cite:
Salah M, Shawky A, Gamal E, Helmy E, Shawkat A, Abdelmoneum RA. Real-Time Intrafraction Motion Management in Magnetic Resonance Imaging-Guided Adaptive Radiotherapy and Its Impact on Treatment Precision. Integr Oncol Diagn Treat. 2026;1(2):108-124. DOI: 10.67692/IODT.26.7900

 DOI: 10.67692/IODT.26.7900

1. Introduction

Magnetic resonance imaging (MRI)-guided adaptive radiotherapy (MRgART) represents a paradigm shift in radiation oncology by integrating diagnostic-quality MRI with therapeutic radiation delivery, enabling continuous soft-tissue visualization before, during, and after beam delivery [1,2]. Unlike conventional image-guided radiotherapy systems that rely on cone-beam computed tomography or kilovoltage imaging for pre-treatment positional verification, MR-Linac technology offers real-time anatomical monitoring throughout the entire treatment fraction, fundamentally transforming the management of intrafraction motion [3].

Intrafraction motion — defined as target and organ displacement occurring during beam delivery — remains one of the principal sources of geometric uncertainty in external beam radiotherapy. This motion arises from multiple mechanisms: respiratory excursion affects thoracic and abdominal targets; gastrointestinal peristalsis, rectal gas fluctuations, and bladder filling alter pelvic organ positions; and involuntary patient movement contributes to positional drift across all anatomical sites [4,5]. Conventional approaches to managing this uncertainty include population-based planning target volume margins, internal target volume concepts derived from four-dimensional computed tomography, and respiratory gating using external surrogates. These strategies fundamentally trade geometric precision for safety, increasing the volume of irradiated normal tissue and limiting the therapeutic ratio.

The clinical significance of MRI-guided motion management is now supported by level 1 evidence. A phase III randomized trial demonstrated that MRI-guided stereotactic body radiotherapy for prostate cancer reduced acute grade 2 or greater genitourinary toxicity from 43.4% to 24.4% ($p = 0.01$) and eliminated acute grade 2 or greater gastrointestinal toxicity compared with computed tomography-guided treatment [6]. Two-year follow-up confirmed these benefits, with late grade 2 or greater genitourinary toxicity reduced by approximately half (27% vs 51%; $p = 0.004$) [7]. These results underscore the clinical impact of resolving intrafraction geometric uncertainty through real-time MRI guidance.

This review aimed to critically evaluate the current state of intrafraction motion management in MRgART, encompassing the technological foundations of available platforms, site-specific motion characteristics, established and investigational management strategies, the clinical evidence base, and comparative performance against conventional image-guided approaches.

2. Materials and Methods

2.1. Literature Search Strategy

A structured narrative review was conducted. PubMed/MEDLINE was systematically searched from inception through March 2026 using the following search terms: (“MR-Linac” OR “MRI-guided radiotherapy” OR “MR-guided radiotherapy” OR “MRgRT” OR “MRgART”) AND (“intrafraction motion” OR “motion management” OR “beam gating” OR “adaptive radiotherapy” OR “cine MRI”). Bibliographies of identified key articles were manually screened to identify additional relevant references.

Inclusion criteria were: peer-reviewed original research articles, prospective registries, randomized controlled trials, phase I/II/III clinical trials, and international consensus documents reporting clinical or technical data on intrafraction motion management in MR-Linac-based radiotherapy. Exclusion criteria were: review articles without original data, conference abstracts lacking full data, studies exclusively reporting MRI-only simulation without actual MR-Linac treatment delivery, and studies limited to the discontinued cobalt-60 MRIdian platform. A total of 47 references met the inclusion criteria and were incorporated in the final synthesis. As this review was based exclusively on published literature, ethics approval and informed consent were not required.

 DOI: 10.67692/IODT.26.7900

3. Results

3.1. Overview of Commercial MR-Linac Platforms

Two MR-Linac systems dominated clinical practice worldwide. The 1.5 T system (Elekta Unity) had surpassed 150 installed systems globally by 2025, with deployments across more than 14 countries on five continents [8,9]. The 0.35 T system (ViewRay MRIdian Linac), operated by the reconstituted ViewRay Systems, Inc. following the parent company's Chapter 11 filing in July 2023, maintained approximately 55–65 operational systems as of 2025 [9]. Their contrasting magnetic field strengths produced fundamentally different imaging-treatment trade-offs that shaped motion management approaches, as summarized in Table 1 (see also Supplementary Figure S1).

3.2. The 1.5 T MR-Linac

The 1.5 T system integrates a modified 1.5 T MRI scanner with a 7 MV flattening-filter-free linear accelerator. Its high field strength yields approximately 4.3-fold greater intrinsic signal-to-noise ratio compared with the 0.35 T system, enabling a comprehensive diagnostic pulse sequence library including T1-weighted, T2-weighted, balanced steady-state free precession, diffusion-weighted imaging, and dynamic contrast-enhanced MRI [10,11]. Real-time cine MRI operated at 5 Hz, alternating between sagittal and coronal planes (effective 2.5 Hz per plane) [12].

Automatic real-time beam gating — achieved through a dedicated motion management module cleared by the United States Food and Drug Administration in February 2023 — uses a template-based deformable registration algorithm that continuously matches each cine frame against a user-defined tracking volume [13]. The gating decision is based on a volume-overlap criterion: beam delivery is paused when predicted overlap between the tracking structure and its gating envelope drops below a user-specified threshold, typically set at 95% [13]. A predictive algorithm compensated for total system latency, reducing effective gating latency from approximately 350 milliseconds to near zero [13]. The treatment planning system supports both an adapt-to-position workflow and an adapt-to-shape workflow [8].

3.3. The 0.35 T MR-Linac

The linac-based 0.35 T MRIdian uses a 6 MV flattening-filter-free linear accelerator (~600 MU/min) on a split-bore 0.345 T ring-gantry architecture, enabling step-and-shoot intensity-modulated radiotherapy. Although lower field strength produced inherently lower signal-to-noise ratio, it conferred clinically important advantages: reduced susceptibility artifacts, minimal chemical shift distortion, and substantially attenuated electron return effects at air–tissue interfaces — approximately 5.5-fold lower than at 1.5 T [15,16]. Sagittal cine MRI operated at 4 frames per second standard. Real-time gating used a boundary-crossing criterion: beam delivery was interrupted when the tracked target contour, propagated by deformable registration from a reference frame, exceeded a clinician-defined spatial boundary on any of the monitored cine planes. The fourth-generation platform extended gating to simultaneous monitoring of up to three orthogonal planes and integrated automated contouring and adaptive steps [12,16]. The original cobalt-60 MRIdian generation was no longer in routine clinical use as of 2025; this review focused on the linac-based platforms exclusively [3,9].

 DOI: 10.67692/IODT.26.7900

Table 1. Technical Comparison of Commercial MR-Linac Platforms (Linac-Based Systems; 2025 Data). Abbreviations: FFF, flattening-filter-free; SNR, signal-to-noise ratio; bSSFP, balanced steady-state free precession; DWI, diffusion-weighted imaging; DCE-MRI, dynamic contrast-enhanced MRI; IMRT, intensity-modulated radiotherapy; VMAT, volumetric modulated arc therapy; DSV, diameter spherical volume; ERE, electron return effect.

Parameter	1.5 T MR-Linac (Elekta Unity)	0.35 T MR-Linac (ViewRay MRIdian Linac/A3i)	Refs
Magnetic field strength	1.5 T	0.35 T	[8,9]
Linear accelerator	7 MV FFF (≤14.5 MU/pulse)	6 MV FFF (~600 MU/min)	[8,9]
Intrinsic SNR	~4.3× higher SNR vs 0.35 T	Baseline; lower SNR but reduced artifacts and ERE	[10]
Available MR pulse sequences	T1w, T2w, bSSFP, DWI, DCE-MRI	bSSFP; limited library vs 1.5 T	[10,11]
Cine MRI frame rate	5 Hz alternating (sagittal + coronal; effective 2.5 Hz per plane)	4 fps standard; up to 8 fps with compressed sensing (A3i)	[12]
Multiplanar monitoring	2 planes (alternating)	Up to 3 planes simultaneously (A3i)	[12]
Gating criterion	Volume-overlap: beam inhibited when overlap with gating envelope falls below threshold (~95%)	Boundary-crossing: beam inhibited when contour exceeds spatial boundary on any monitored plane	[8,9,13]
FDA clearance (gating)	February 2023 (motion management module)	2014 (Co-60); 2017 (linac)	[13]
Effective beam-off latency	~350 ms raw; ~zero with predictive algorithm	~250 ms (linac)	[13]
Online adaptive workflows	Adapt-to-Position (ATP); Adapt-to-Shape (ATS)	On-table replanning with auto-contouring and re-optimization	[8]
Beam delivery mode	Step-and-shoot IMRT (7 or 9 fixed beams)	Step-and-shoot IMRT	[8,9]
VMAT	Research only	Not available	[14]
Geometric distortion	<1 mm within 300 mm DSV; ~2.5 mm at 500 mm DSV	Lower distortion (lower field)	[11]
ERE	14–24% skin dose increase at air–tissue interfaces	~5.5× lower ERE vs 1.5 T	[15,16]
Approximate installed base (2025)	>150 systems worldwide	~55–65 operational systems	[9]

3.4. Technical Limitations Common to Both Platforms

Critical technical limitations affected both platforms. Neither supported volumetric modulated arc therapy or noncoplanar beam arrangements in routine clinical practice; treatment was limited to step-and-shoot intensity-modulated radiotherapy. On the 1.5 T system, geometric distortions remained sub-millimeter within a 300-mm diameter spherical volume but reached approximately 2.5 mm at 500-mm diameter, necessitating careful quality assurance for peripheral targets [11]. The electron return effect increased skin dose by 14% to 24% at 1.5 T [15,16]. Both platforms imposed patient eligibility restrictions of approximately 5% to 10% owing to standard MRI contraindications.

 DOI: 10.67692/IODT.26.7900

3.5. Patterns of Intrafraction Motion by Tumor Site

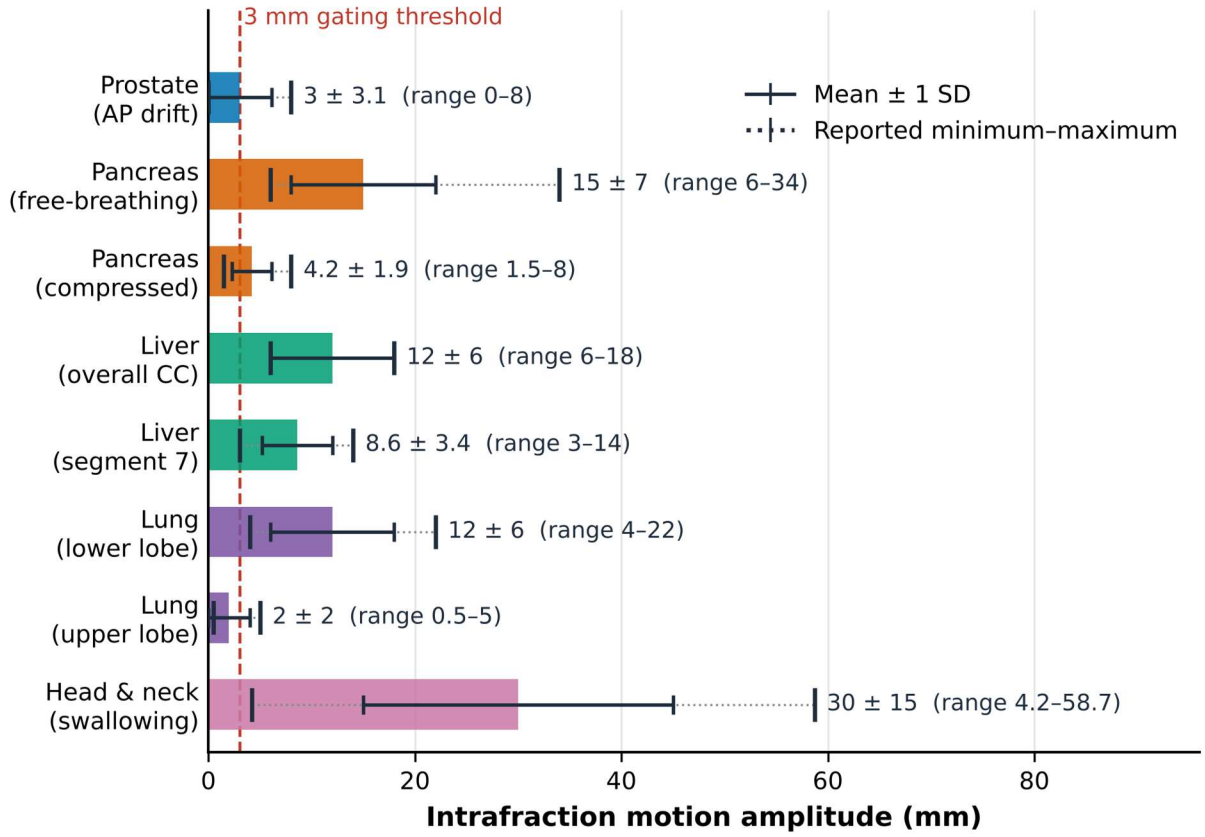
A quantitative summary of site-specific intrafraction motion characteristics as characterized by cine MRI on MR-Linac platforms is provided in Table 2 and illustrated in Figure 1.

Table 2. Site-Specific Intrafraction Motion Characteristics as Characterized by Cine MRI on MR-Linac Platforms. Abbreviations: AP, anterior-posterior; SI, superior-inferior; LR, left-right; CC, craniocaudal; OAR, organs at risk; GI, gastrointestinal; PTV, planning target volume; ITV, internal target volume.

Tumor Site	Dominant Motion Type	Primary Direction	Amplitude / Margin Data	Key Drivers	Refs
Prostate	Gradual drift	Anterior-posterior	AP: 1.8±3.1 mm; SI: 1.7±2.6 mm PTV margins: LR 1.8/AP 3.2/SI 2.9 mm	Rectal gas; bladder filling; patient relaxation	[4,17]
Pancreas	Respiratory + baseline drift + organ deformation	Craniocaudal	Free-breathing CC: 15 mm (range 6–34) With abdominal compression: 4.2±1.9 mm OAR deformation: 5.5–8.2 mm (max >37 mm)	Respiration; peristalsis; GI filling	[5,18,19]
Liver	Respiratory	Craniocaudal	CC: 6–18 mm (varies by segment) Segment 7: 8.6±3.4 mm Diaphragm–tumor correlation r=0.97±0.04	Respiration; hepatic segment location	[20,21]
Lung	Respiratory ± cardiac pulsation	Craniocaudal	Lower lobe: 12±6 mm Upper lobe/chest wall: 2±2 mm PTV reduction vs ITV: >46%	Respiration (location-dependent); cardiac pulsation	[22,23,24]
Head and Neck	Transient swallowing + setup drift	Superior-inferior	Swallowing peak: up to 58.7 mm (larynx) PTV margins required: 4.1–7.7 mm (subsite-dependent)	Swallowing; progressive anatomical change	[25]

 DOI: 10.67692/IODT.26.7900

Figure 1. Quantitative Intrafraction Motion Amplitudes by Tumor Site. Bar graph depicting mean intrafraction motion amplitudes (mm) by tumor site and primary direction, as characterized by cine MRI on MR-Linac platforms. Error bars represent ±1 standard deviation where reported in source studies. The horizontal dashed reference line at 3 mm indicates the standard clinical gating threshold. Head-and-neck values represent peak transient swallowing displacements, not continuous motion amplitudes. Source references: prostate [4,17]; pancreas [5,18]; liver [20,21]; lung [22,23]; head and neck [25].



3.5.1. Prostate

Prostate intrafraction motion was dominated by gradual drift along the anterior-posterior axis, driven primarily by rectal gas dynamics and bladder filling. On the 1.5 T MR-Linac, prostate motion at the start of treatment sessions was characterized by anterior displacement of 1.8 ± 3.1 mm and superior displacement of 1.7 ± 2.6 mm, relaxing over 12 to 15 minutes before transitioning to random motion [4]. Achievable planning target volume margins were 1.8 mm (left-right), 3.2 mm (anterior-posterior), and 2.9 mm (superior-inferior) — substantially smaller than the 4 to 5 mm margins standard with cone-beam computed tomography guidance [4]. Large intrafraction excursions were stochastic, with 63.2% of patients experiencing at least one fraction with suboptimal geometric dose coverage, and inferior-posterior motion was associated with significantly higher grade 2 genitourinary toxicity (66.7% vs 13.9%; p = 0.001) [17].

3.5.2. Pancreas

Pancreatic tumors exhibited among the most challenging motion profiles, combining respiratory excursion with baseline drift and surrounding organ deformation. Free-breathing craniocaudal amplitude averaged 15 mm (range, 6–34 mm) [5], although abdominal compression reduced this by approximately 50% to 4.2 ± 1.9 mm [18]. Gastrointestinal organs

 DOI: 10.67692/IODT.26.7900

at risk underwent median intrafraction deformations of 5.5 to 8.2 mm, with maximum excursions exceeding 37 mm, often shifting from low-dose to high-dose regions during treatment — a finding invisible without real-time MRI that fundamentally justified intrafraction monitoring in pancreatic stereotactic body radiotherapy [19].

3.5.3. Liver

Liver tumors demonstrated respiratory-driven craniocaudal motion of 6 to 18 mm varying by hepatic segment, with posterior-lateral segments exhibiting the largest excursions at 8.6 ± 3.4 mm [20]. The diaphragm dome served as an excellent surrogate for liver tumor motion (correlation coefficient r = 0.97 ± 0.04) across 305,644 cine MR frames from 118 treatment sessions on a 0.35 T MR-Linac, validating surrogate use when tumor contrast was suboptimal [21].

3.5.4. Lung

Lung tumor motion depended strongly on anatomical location: lower-lobe tumors exhibited craniocaudal amplitudes of 12 ± 6 mm, whereas upper-lobe and chest wall-attached tumors moved only 2 ± 2 mm [22]. MR-guided gating reduced planning target volume volumes to less than 54% of internal target volume-based volumes derived from four-dimensional computed tomography, dramatically reducing irradiated lung volumes [23,24].

3.5.5. Head and Neck

Head-and-neck tumors presented a distinct motion challenge: swallowing produced transient but potentially large displacements of up to 58.7 mm superiorly for the larynx, superimposed on slower setup drift. Accounting for swallowing-related motion required planning target volume margins of 4.1 to 7.7 mm depending on subsite and direction — exceeding the 3 to 5 mm margins commonly used [25].

3.6. Motion-Management Strategies in MRgART

The principal motion-management strategies currently employed in MRgART are summarized in Table 3. These strategies spanned four hierarchical levels of technological sophistication: real-time beam gating (current standard of care), online adaptive replanning, real-time multileaf collimator tracking (research stage), and artificial intelligence-assisted motion forecasting (investigational). The overall workflow is illustrated in Supplementary Figure S2.

3.7. Real-Time Beam Gating

Real-time beam gating was the most widely implemented motion management approach in MRgART. On both platforms, two-dimensional cine MRI continuously monitored target position during beam delivery, automatically pausing irradiation when the target exceeded predefined spatial boundaries, typically 3 mm for most clinical applications. The gating criterion differed between platforms (see Sections 3.2 and 3.3). Gated delivery reduced mean two-dimensional root-mean-square target displacement from 8.3 ± 4.3 mm (ungated) to 1.6 ± 0.6 mm (gated) in liver and lung stereotactic body radiotherapy [26]. Gating duty cycles ranged from 41% to 93% between patients (mean 55–72%) [27]. Visual biofeedback coaching reduced beam-off time by approximately 34% and beam-off events by 57% [34]. Increasing the contour excursion threshold from 0% to 5% improved beam duty cycle from 19.5% to 60.8% with acceptable gross tumor volume coverage [35].

 DOI: 10.67692/IODT.26.7900

Table 3. Current Motion-Management Strategies in Magnetic Resonance Imaging-Guided Adaptive Radiotherapy. Abbreviations: MLC, multileaf collimator; SBRT, stereotactic body radiotherapy; LSTM, long short-term memory; RMSE, root-mean-square error; QA, quality assurance; GTV, gross tumor volume; CTV, clinical target volume; OAR, organs at risk.

Strategy	Mechanism	Strengths	Limitations	Clinical Status	Refs
Real-time beam gating	Cine MRI monitors target; beam automatically interrupted when target exceeds predefined spatial boundary	2D RMS displacement: 8.3±4.3 →1.6±0.6 mm; clinically validated; adjustable thresholds; available on both platforms	Duty cycle 41–93% (mean 55–72%); extended treatment time; 2D monitoring only; gating latency 50–436 ms	Routine clinical use on both 1.5 T and 0.35 T platforms	[13,26,27]
Real-time MLC tracking	MLC leaves continuously follow tumor motion without beam interruption	Near 100% duty cycle; sub-millimeter tracking accuracy; 93% gamma pass rate (2%/2 mm) for lung SBRT	Not clinically available; complex control system; requires extensive QA; regulatory pathway unresolved	Research only; proof-of-concept on 1.5 T MR-Linac	[14,28]
Online adaptive replanning	Daily 3D MRI; contours deformably propagated; plan fully re-optimized before delivery	84.4% of fractions benefit from adaptation; improved GTV/CTV near-minimum dose; reduced OAR dose	Addresses interfraction (not real-time) changes; session 39–75 min; requires physician and physicist presence; learning curve	Routine on both platforms	[8,29,30]
AI-assisted motion forecasting	Deep learning models (LSTM, transformer) predict tumor position 250–500 ms ahead	RMSE 0.7–0.9 mm; inference 8–36 ms; patient-specific training from ≥8 cine frames	Not clinically deployed; extensive prospective validation required; regulatory approval process unresolved	Investigational; TrackRAD2025 benchmarking ongoing	[31,32,33]

3.8. Real-Time Multileaf Collimator Tracking

Real-time multileaf collimator tracking — in which collimator leaves continuously followed tumor motion — offered the theoretical advantage of high duty cycles without beam interruption. Proof-of-concept studies on the 1.5 T MR-Linac demonstrated tracking accuracy within 0.04 ± 0.36 mm for the imaging component and sub-millimeter accuracy for the collimator component, with 93% gamma pass rates at 2%/2 mm for lung stereotactic body radiotherapy incorporating volumetric modulated arc therapy [14]. For prostate drift correction,

 DOI: 10.67692/IODT.26.7900

collimator tracking improved gamma pass rates from 21% (untracked) to 89–91% at 2%/2 mm criteria. Despite these results, multileaf collimator tracking remained exclusively in the research domain on both platforms.

3.9. Online Adaptive Replanning

Online adaptive replanning addressed interfraction anatomical changes. The adapt-to-shape workflow on the 1.5 T system involved acquiring a daily three-dimensional MRI, deformably propagating contours, physician review and editing, full plan re-optimization with Monte Carlo dose calculation, independent quality assurance verification, and position verification before delivery [8]. Across 265 adapted fractions on the 0.35 T system, 84.4% required adaptation, with significant improvements in gross tumor volume/clinical target volume near-minimum dose and reduced organ-at-risk exposure across liver, lung, lymph node, and pancreatic subgroups [29]. Adapt-to-shape sessions averaged 39 to 48 minutes for most sites, with learning curves reducing this by 4 to 8 minutes [30].

3.10. Artificial Intelligence-Assisted Motion Forecasting

Artificial intelligence-assisted motion forecasting addressed the latency between motion detection and beam response. Long short-term memory recurrent neural networks achieved three-dimensional tumor position prediction at 280-millisecond latency with mean root-mean-square error of 0.9 mm across 158 datasets from 46 patients [32], while external validation demonstrated root-mean-square error of 0.139 at 500-millisecond prediction horizons with inference times of 5 milliseconds [33]. Transformer-based deformable tracking frameworks trained on more than 1.4 million cine-MRI frames achieved median Dice similarity coefficient of 0.92 and centroid root-mean-square error below 1 mm at inference times of 8 to 36 milliseconds [31]. None of these methods had yet been clinically deployed on commercial MR-Linac systems.

3.11. Clinical Evidence and Outcomes

A summary of key clinical studies is provided in Table 4.

3.11.1. Prostate Cancer

A phase III randomized trial randomized 156 prostate cancer patients to MRI-guided (0.35 T system, 2-mm planning target volume margins) versus computed tomography-guided (4-mm margins) stereotactic body radiotherapy at 40 Gy in 5 fractions [6,7]. The primary endpoint was met: acute grade 2 or greater genitourinary toxicity was 24.4% versus 43.4% ($p = 0.01$), and acute grade 2 or greater gastrointestinal toxicity was 0% versus 10.5% ($p = 0.003$). Two-year follow-up demonstrated durable benefit: cumulative late grade 2 or greater genitourinary toxicity was 27% versus 51% ($p = 0.004$), with significantly better patient-reported bowel function (odds ratio, 0.44; $p = 0.035$) and sexual function (odds ratio, 0.37; $p = 0.03$) favoring MRI guidance [7]. Daily adaptive replanning was not performed in this trial; the benefits derived primarily from superior soft-tissue visualization enabling tighter margins and real-time gating (Figure 2). A 200-patient single-institution series confirmed 99% prostate-specific antigen response rates with low toxicity profiles [42].

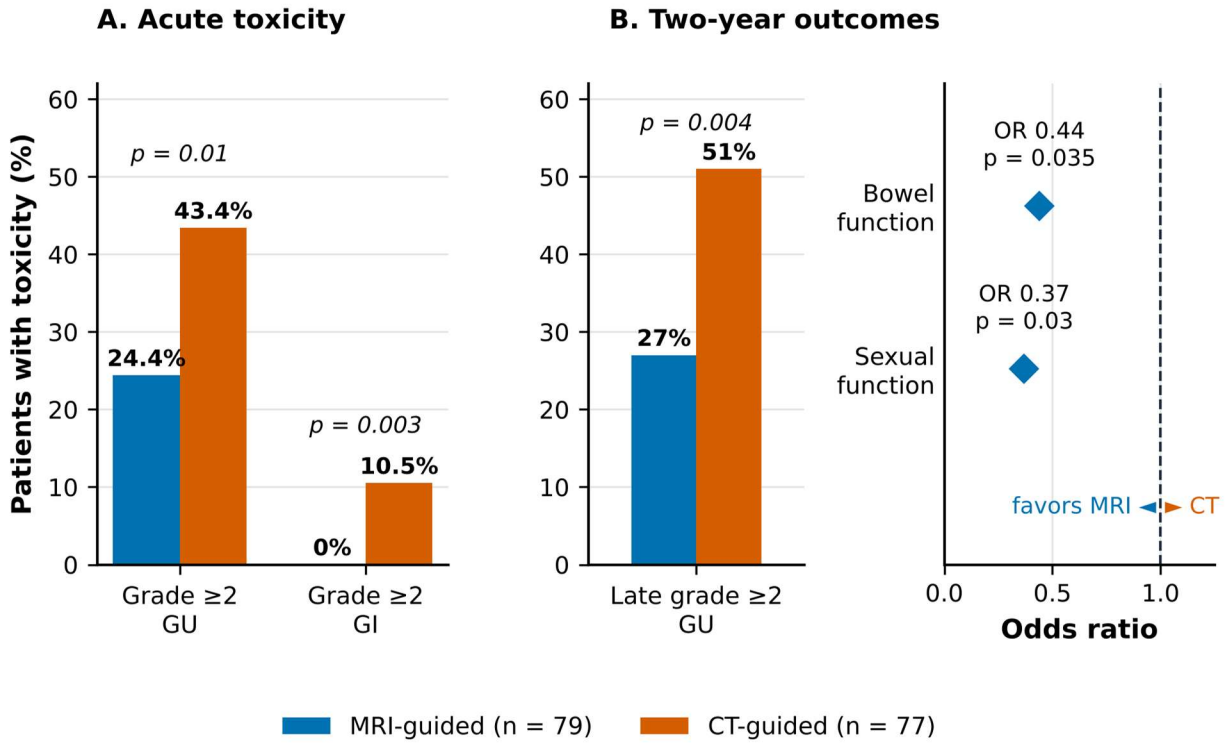
 DOI: 10.67692/IODT.26.7900

Table 4. Summary of Key Clinical Evidence for Magnetic Resonance Imaging-Guided Adaptive Radiotherapy With Motion Management. Abbreviations: RCT, randomized controlled trial; GU, genitourinary; GI, gastrointestinal; LC, local control; OS, overall survival; LPFS, local progression-free survival; FFLP, freedom from local progression; LAPC, locally advanced pancreatic cancer; BRPC, borderline-resectable pancreatic cancer; BED_{10}, biologically effective dose (α/β = 10 Gy); OR, odds ratio; QoL, quality of life; PSA, prostate-specific antigen; fx, fractions; mo, months; yr, years; dx, diagnosis.

Study	Design	Site	N	Dose / Platform	Efficacy	Toxicity
Kishan et al [6,7] JAMA Oncol 2023; Eur Urol 2025	Phase III RCT Single center	Prostate (localized)	156	40 Gy/5 fx MRI arm: 2 mm PTV CT arm: 4 mm PTV	2-yr late GU ≥2: 27% vs 51% (p=0.004) Bowel QoL: OR 0.44 (p=0.035) Sexual QoL: OR 0.37 (p=0.03)	Acute GU ≥2: 24.4% vs 43.4% (p=0.01) Acute GI ≥2: 0% vs 10.5% (p=0.003)
Parikh et al [36]; Chuong et al [37] IJROBP 2023; Radiother Oncol 2024	Phase II Multi-center	Pancreas (LAPC/BRPC)	136	50 Gy/5 fx (BED_{10}=100 Gy) 0.35 T; adaptive + gating	2-yr LC: 78.2% Median OS from dx: 22.8 mo 2-yr OS from dx: 53.6%	Acute GI ≥3 (definite): 0% Late GI ≥3 (definite): 0% (probable: 4.6%)
Rudra et al [38] Cancer Med 2019	Retrospective Multi-center	Pancreas (inoperable)	44	High-dose (BED_{10}>70 Gy) vs standard	2-yr OS: 49% vs 30% (p=0.03) Dose-response confirmed	0% grade ≥3 GI in high-dose cohort
van Dams et al [39]; Henke et al [40]	Phase I/Retrospective Multi-center	Liver (primary/mets)	26/20	SBRT; BED_{10} ≥100 Gy preferred	FFLP: 80.4% 2-yr LC: 96% (BED_{10} ≥100 Gy)	Acceptable; no grade ≥4 events
Hering et al [41] Strahlenther Onkol 2024	Retrospective Single center	Lung (central/ultracentral)	64 pts 92 lesions	MR-guided adaptive SBRT	1-yr LPFS: 96.3%	0% grade ≥3 toxicity
Gelbart Pridan et al [42] Front Oncol 2023	Retrospective Single center	Prostate	200	SBRT on MR-Linac	99% PSA response	Low toxicity profile

 DOI: 10.67692/IODT.26.7900

Figure 2. Clinical Outcomes of Magnetic Resonance Imaging-Guided Versus Computed Tomography-Guided Prostate Stereotactic Body Radiotherapy: Phase III Randomized Trial. Summary of toxicity and patient-reported outcomes (N = 156). Panel A (Acute Toxicity): Grouped bar chart comparing proportions with grade ≥2 genitourinary and gastrointestinal toxicity in the MRI-guided arm (0.35 T system, 2-mm planning target volume margins) versus the CT-guided arm (4-mm margins). Panel B (Two-Year Outcomes): late toxicity rates and patient-reported outcome odds ratios at 2-year follow-up. Cumulative late genitourinary ≥2: 27% vs 51% (p = 0.004); bowel function odds ratio: 0.44; sexual function odds ratio: 0.37. An odds ratio less than 1 indicates lower odds of the adverse outcome in the MRI-guided arm. Source references: [6,7].



3.11.2. Pancreatic Cancer

A multi-institutional phase II trial enrolled 136 patients with locally advanced or borderline-resectable pancreatic cancer, delivering 50 Gy in 5 fractions (biologically effective dose$_{10}$ = 100 Gy) on the 0.35 T system with daily adaptive replanning and real-time gating [36]. The primary safety endpoint was met: 0% acute grade 3 or greater gastrointestinal toxicity definitively attributable to treatment. At mature follow-up, median overall survival was 22.8 months from diagnosis; 2-year overall survival from diagnosis was 53.6%; late grade 3 or greater definitively related gastrointestinal toxicity remained at 0% (probably related: 4.6%) [37]. A multi-institutional retrospective analysis demonstrated a dose-response relationship: patients receiving biologically effective dose$_{10}$ greater than 70 Gy achieved 2-year overall survival of 49% versus 30% for standard-dose regimens (p = 0.03), with zero grade 3 or greater gastrointestinal toxicity in the high-dose cohort [38]. A 13-center international consensus protocol for 1.5 T MR-Linac pancreatic stereotactic body radiotherapy has since been established [43].

3.11.3. Liver Cancer

MR-guided liver stereotactic body radiotherapy enabled fiducial-free treatment with direct

 DOI: 10.67692/IODT.26.7900

tumor visualization and gated delivery. Multi-institutional data reported freedom from local progression of 80.4% across 26 patients [39]. Phase I prospective data demonstrated 2-year local control of 79.6% overall, increasing to 96% when biologically effective dose$_{10}$ of 100 Gy or greater was achieved, establishing a clear dose-response relationship enabled by safe dose escalation under MRI guidance [40]. Phase III randomized evidence is being generated through an ongoing international trial (NCT06362395).

3.11.4. Lung Cancer

Lung stereotactic body radiotherapy outcomes were notable for central and ultracentral tumors, where conventional approaches carry substantial risk. One-year local progression-free survival of 96.3% and zero grade 3 or greater toxicity were reported across 64 patients and 92 lesions treated with MR-guided adaptive stereotactic body radiotherapy [41]. MR-guided gating reduced planning target volume volumes to less than 54% of internal target volume-based volumes, enabling ablative doses with markedly improved therapeutic ratios [24].

3.12. Comparative Perspective: MRI-Guided Versus Cone-Beam Computed Tomography-Based Motion Management

The comparative landscape between MR-guided and cone-beam computed tomography-based motion management was characterized by a fundamental trade-off: superior imaging and real-time motion management capabilities versus workflow efficiency and acquisition cost. A comprehensive comparison is provided in Supplementary Table S1.

Cone-beam computed tomography provided only pre-treatment snapshot imaging with limited soft-tissue contrast, correcting for interfraction positional changes but offering no intrafraction monitoring capability. Artificial intelligence-driven online adaptive replanning on cone-beam computed tomography platforms achieved session times of 15 to 20 minutes with automated contouring and re-optimization; however, these systems could not visualize the tumor in real time during beam delivery and were fundamentally limited in soft-tissue contrast compared with MRI.

Fiducial-based tracking systems provided real-time intrafraction position data at approximately 10 Hz with localization accuracy within 2 mm [28]. However, fiducials required invasive implantation carrying risks of bleeding, infection, and migration; they served as position surrogates rather than providing direct tumor visualization; and they could not detect organ deformation or volume changes [28]. MRI eliminated fiducial dependence entirely while providing richer anatomical information. The evidence favoring MRI guidance was strongest for sites where soft-tissue contrast was critical and motion was substantial, including the pancreas, liver, and prostate.

4. Discussion

This review evaluated the current state of real-time intrafraction motion management in MRgART across two commercial MR-Linac platforms. The strongest evidence was identified for prostate stereotactic body radiotherapy, where a phase III randomized trial demonstrated halved late toxicity through margin reduction enabled by real-time MRI guidance, and for pancreatic stereotactic body radiotherapy, where daily adaptation and gating permitted ablative doses with near-zero severe gastrointestinal toxicity and median overall survival exceeding 22 months from diagnosis.

4.1. Technical and Workflow Barriers

Treatment session duration averaged 48 minutes across anatomical sites, with pancreatic

 DOI: 10.67692/IODT.26.7900

stereotactic body radiotherapy sessions reaching a median of 75.5 minutes on the 1.5 T MR-Linac, compared with 15 to 20 minutes for conventional linac treatments [30]. This limited daily throughput to approximately 6 to 10 patients per machine, compared with 20 to 30 for conventional systems. Learning curves improved throughput significantly: one center reported increasing from 7.6 to 13.9 fractions per day over 24 months [30]. Patient eligibility restrictions affected approximately 5% to 10% of potential candidates because of MRI contraindications, claustrophobia, or body habitus incompatible with the 70-cm bore.

4.2. Training and Staffing Requirements

Staffing requirements were substantially higher than for conventional radiotherapy. Recommended core teams include 6 to 8 dedicated radiation therapists alongside MR physicists and physicians available for real-time contouring decisions at each fraction [30]. The convergence of diagnostic MRI expertise and therapeutic radiation delivery has created a training gap — a consequence of the historical separation between diagnostic and therapeutic radiology. Institutions must invest in cross-disciplinary education covering MR safety, adaptive workflow management, and online contouring quality assurance [44].

4.3. Cost and Resource Implications

MR-Linac systems cost approximately $10 to $15 million to acquire, with specialized vault construction adding substantially. Health economic analyses indicated that MR-Linac prostate stereotactic body radiotherapy approached cost-effectiveness versus conventional 5-fraction stereotactic body radiotherapy only when complication rates were reduced by 54% or more [45]. An open-access decision-analytic framework provided context-specific cost modeling, using €80,000 per quality-adjusted life year as a base-case threshold, recognizing that cost-effectiveness varied substantially by tumor site, healthcare system, and local reimbursement [45]. The commercial restructuring of the 0.35 T platform manufacturer in 2023 to 2024 introduced additional uncertainty regarding service continuity and software updates for operators, which institutions must factor into long-term investment planning.

4.4. Evidence Gaps and Standardization

A single completed phase III randomized controlled trial exists, limited to a single center and single tumor site. Most published data originated from prospective registries — the MOMENTUM study encompassed more than 3,500 patients across 34 indications at more than 17 centers [46] — single-arm prospective trials, and retrospective series. Protocol heterogeneity across institutions complicated data aggregation: centers varied in planning target volume margins, adaptive workflow triggers, gating thresholds, and contouring approaches. Failure mode analysis identified 279 potential failure modes in the MRgART workflow, 31 classified as high risk [44]. ICRU Report 97 provided a foundational framework for MR-guided radiotherapy standardization, but broader adoption of uniform protocols remained a priority [47].

4.5. Future Directions

Several converging developments are expected to shape the trajectory of intrafraction motion management. Artificial intelligence-assisted auto-segmentation is projected to compress adaptive workflow times below 20 minutes; patient-specific deep learning models already achieved accurate localization from as few as 8 training frames [31]. Long short-term memory and transformer-based motion prediction networks demonstrating sub-millimeter accuracy at clinically relevant latencies could enable prospective multileaf collimator tracking, potentially eliminating gating efficiency losses entirely [32,33]. Volumetric modulated arc therapy

 DOI: 10.67692/IODT.26.7900

implementation, currently demonstrated in research on the 1.5 T system, would substantially improve dose conformality and delivery efficiency [14]. Critically, multi-institutional phase III trials comparing MR-guided with best-available conventional approaches across pancreas, liver, lung, and head-and-neck sites are urgently needed, and cost-effectiveness must be demonstrated with prospective data. Standardized protocols and quality-assurance frameworks must be developed and internationally harmonized through collaborations such as the MOMENTUM consortium and the MR-Linac Consortium [46,47].

In conclusion, MRI-guided intrafraction motion management transitioned from technological novelty to clinical necessity for specific treatment scenarios. The evidence was most compelling for prostate, pancreatic, and central lung stereotactic body radiotherapy. The essential insight from the first decade of clinical MR-Linac experience was not that MRI guidance was universally superior but that it was selectively transformative — enabling treatments previously impossible or unacceptably toxic. Distinguishing between the two commercially available platforms, each with distinct field strengths, gating mechanisms, installed bases, and regulatory trajectories, was critical for accurate interpretation of the literature and appropriate clinical adoption. The research imperative was to define precisely where the selective advantage of real-time MRI guidance justified the substantial investment required and to develop the technological and clinical infrastructure that made MRgART accessible, efficient, and reproducible across institutions worldwide.

Disclosures

Funding: None.

Ethical approval: Not applicable.

Conflicts of interest: All authors declare no conflict of interest.

Use of AI tools: Artificial intelligence tools were used for grammar correction and text reformatting. No generative AI was used for data extraction, interpretation of findings, or critical appraisal.

Authors contribution:

- **Manar Salah:** Conceptualization, Methodology, Investigation, Writing – Original Draft, Project Administration.
- **Ahmed Shawky:** Conceptualization, Methodology, Validation, Writing – Review & Editing.
- **Eman Gamal:** Investigation, Data Curation, Visualization, Writing – Original Draft.
- **Eman Helmy:** Investigation, Formal Analysis, Validation, Writing – Review & Editing.
- **Alaa Shawkat:** Methodology, Resources, Visualization, Writing – Review & Editing.
- **Rasha Adel Abdelmoneum:** Supervision, Validation, Writing – Review & Editing.

All authors contributed to the manuscript, critically reviewed its intellectual content, approved the final version for publication, and agreed to be accountable for their respective contributions.

References

[1] Lagendijk JJ, Raaymakers BW, van Vulpen M. The magnetic resonance imaging-linac system. Semin Radiat Oncol. 2014;24:207-9. https://doi.org/10.1016/j.semradonc.2014.02.009

[2] Raaymakers BW, Lagendijk JJ, Overweg J, et al. Integrating a 1.5 T MRI scanner with a 6 MV accelerator: proof of concept. Phys Med Biol. 2009;54:N229-37. https://doi.org/10.1088/0031-9155/54/12/N01

[3] Mutic S, Dempsey JF. The ViewRay system: magnetic resonance-guided and controlled radiotherapy. Semin Radiat Oncol. 2014;24:196-9. https://doi.org/10.1016/j.semradonc.2014.02.008

[4] Willigenburg T, Zachiu C, Asselen BV, et al. Prostate motion in magnetic resonance imaging-guided

 DOI: 10.67692/IODT.26.7900

radiotherapy and its impact on margins. Strahlenther Onkol. 2024;200:412-21. https://doi.org/10.1007/s00066-023-02136-5

[5] Heerkens HD, van Vulpen M, van den Berg CA, et al. MRI-based tumor motion characterization and gating schemes for radiation therapy of pancreatic cancer. Radiother Oncol. 2014;111:252-7. https://doi.org/10.1016/j.radonc.2014.03.002

[6] Kishan AU, Ma TM, Lamb JM, et al. Magnetic resonance imaging-guided vs computed tomography-guided stereotactic body radiotherapy for prostate cancer: the MIRAGE randomized clinical trial. JAMA Oncol. 2023;9:365-73. https://doi.org/10.1001/jamaoncol.2022.6558

[7] Kishan AU, Ma TM, Lamb JM, et al. Magnetic resonance imaging versus computed tomography guidance for stereotactic body radiotherapy in prostate cancer: 2-year outcomes from the MIRAGE randomized clinical trial. Eur Urol. 2025;87:288-96. https://doi.org/10.1016/j.eururo.2024.10.007

[8] Winkel D, Bol GH, Kroon PS, et al. Adaptive radiotherapy: the Elekta Unity MR-linac concept. Clin Transl Radiat Oncol. 2019;18:54-9. https://doi.org/10.1016/j.ctro.2019.04.001

[9] Kluter S. Technical design and concept of a 0.35 T MR-Linac. Clin Transl Radiat Oncol. 2019;18:98-101. https://doi.org/10.1016/j.ctro.2019.05.001

[10] Kooreman ES, van Houdt PJ, Nowee ME, et al. Feasibility and accuracy of quantitative imaging on a 1.5 T MR-linear accelerator. Radiother Oncol. 2019;133:156-62. https://doi.org/10.1016/j.radonc.2019.01.011

[11] Snyder KC, Kim J, Zhao B, et al. Commissioning of a 1.5T Elekta Unity MR-linac: a single institution experience. J Appl Clin Med Phys. 2020;21:160-72. https://doi.org/10.1002/acm2.12944

[12] Charters JA, Bertholet J, Keiper TD, et al. Characterization of real-time multi-planar MRI acquisition parameters for MR-guided radiotherapy. J Appl Clin Med Phys. 2022;23:e13544. https://doi.org/10.1002/acm2.13544

[13] Rusu IM, van Zijp HM, Philippens MEP, et al. Characterizing the motion management system accuracy on a 1.5T MR-Linac. Phys Med. 2025;131:104908. https://doi.org/10.1016/j.ejmp.2025.104908

[14] Uijtewaal P, Borman PTS, Woodhead PL, et al. First experimental demonstration of VMAT combined with MLC tracking for single and multi fraction lung SBRT on an MR-linac. Radiother Oncol. 2023;181:109488. https://doi.org/10.1016/j.radonc.2023.109488

[15] Steciw S. Dose perturbations at tissue interfaces during parallel linac-MR treatments: the lateral scatter electron return effect. Med Phys. 2024;51:7468-79. https://doi.org/10.1002/mp.17331

[16] Xia W, Zhang K, Li M, et al. Electron return effect in MR-guided radiotherapy: Monte Carlo simulation study. Front Oncol. 2020;10:611845. https://doi.org/10.3389/fonc.2020.611845

[17] Kishan AU, Lamb JM, Jani SS, et al. Quantifying intrafraction motion and the impact of gating for magnetic resonance imaging-guided stereotactic radiation therapy for prostate cancer: analysis of the MIRAGE phase 3 randomized trial. Int J Radiat Oncol Biol Phys. 2024;118:1028-38. https://doi.org/10.1016/j.ijrobp.2023.09.046

[18] Grimbergen G, van der Horst A, Winkel D, et al. Intrafraction pancreatic tumor motion patterns during ungated magnetic resonance guided radiotherapy with an abdominal corset. Phys Imaging Radiat Oncol. 2022;21:1-6. https://doi.org/10.1016/j.phro.2021.12.001

[19] Tyagi N, Liang J, Burleson S, et al. Inter- and intrafraction motion assessment and accumulated dose quantification of upper gastrointestinal organs during MR-guided ablative radiation therapy of pancreas patients. Phys Imaging Radiat Oncol. 2022;21:54-60. https://doi.org/10.1016/j.phro.2022.01.002

[20] Tsai YL, Wu SW, Hsu SM, et al. Quantitative analysis of respiration-induced motion of each liver segment with helical computed tomography and 4-dimensional computed tomography. Radiat Oncol. 2018;13:58. https://doi.org/10.1186/s13014-018-1006-5

 DOI: 10.67692/IODT.26.7900

[21] Mao W, Mou B, Liu C, et al. Association between internal organ/liver tumor and external surface motion from cine MR images on an MRI-Linac. Front Oncol. 2022;12:868076. https://doi.org/10.3389/fonc.2022.868076

[22] Seppenwoolde Y, Shirato H, Kitamura K, et al. Precise and real-time measurement of 3D tumor motion in lung due to breathing and heartbeat, measured during radiotherapy. Int J Radiat Oncol Biol Phys. 2002;53:822-34. https://doi.org/10.1016/s0360-3016(02)02803-1

[23] Finazzi T, Palacios MA, Spoelstra FOB, et al. Role of on-table plan adaptation in MR-guided ablative radiation therapy for central lung tumors. Int J Radiat Oncol Biol Phys. 2019;104:933-41. https://doi.org/10.1016/j.ijrobp.2019.03.010

[24] Finazzi T, van Sornsen de Koste JR, Palacios MA, et al. Delivery of magnetic resonance-guided single-fraction stereotactic lung radiotherapy. Phys Imaging Radiat Oncol. 2020;14:17-23. https://doi.org/10.1016/j.phro.2020.04.003

[25] Chan RW, Fatania K, Engstrom C, et al. Cine MRI-based analysis of intrafractional motion in radiation treatment planning of head and neck cancer patients. Radiother Oncol. 2023;185:109738. https://doi.org/10.1016/j.radonc.2023.109738

[26] Ehrbar S, Johl A, Kuhni M, et al. MR-guided beam gating: residual motion, gating efficiency and dose reconstruction for stereotactic treatments of the liver and lung. Radiother Oncol. 2022;174:101-7. https://doi.org/10.1016/j.radonc.2022.07.009

[27] Kluter S, Katayama S, Ghamdi SSA, et al. First prospective clinical evaluation of feasibility and patient acceptance of magnetic resonance-guided radiotherapy in Germany. Strahlenther Onkol. 2020;196:691-8. https://doi.org/10.1007/s00066-020-01578-9

[28] Keall PJ, Nguyen DT, O'Brien R, et al. The safe clinical implementation of MLC tracking in radiotherapy: AAPM Task Group 264 Report. Med Phys. 2021;48:e283-320. https://doi.org/10.1002/mp.14993

[29] Rosenberg SA, Henke LE, Shaverdian N, et al. Dose/volume metric benefit of MR-guided online adaptive radiotherapy in different tumor entities: liver, lung, abdominal lymph nodes, pancreas and prostate. Radiat Oncol. 2022;17:53. https://doi.org/10.1186/s13014-022-02019-8

[30] Leon LM, Smith WL, Roumeliotis M. Treatment time and learning curve analysis of 1.5 T MR-Linac workflows led by radiation oncologists or therapists. Clin Transl Radiat Oncol. 2024;48:100803. https://doi.org/10.1016/j.ctro.2024.100803

[31] Lombardo E, Dhont J, Page D, et al. Patient-specific daily updated deep learning auto-segmentation for MRI-guided adaptive radiotherapy. Radiother Oncol. 2024;191:109969. https://doi.org/10.1016/j.radonc.2023.109969

[32] Yun J, Yip E, Gabos Z, et al. A deep-learning based 3D tumor motion prediction for MR-guided radiotherapy. Int J Radiat Oncol Biol Phys. 2019;105:S233-4. https://doi.org/10.1016/j.ijrobp.2019.06.843

[33] Lin Y, Shao A, Glide-Hurst CK. Towards real-time respiratory motion prediction based on long short-term memory neural networks. Phys Med Biol. 2019;64:085010. https://doi.org/10.1088/1361-6560/ab138f

[34] Kim J, Park J, Wu HG, et al. Visual biofeedback for respiratory motion management in MR-guided radiation therapy. Med Phys. 2017;44:5669-79. https://doi.org/10.1002/mp.12516

[35] Dong P, Lee P, Ruan D, et al. Dose/volume metric impact of distinct gating strategies in cine MR image-guided breath-hold pancreatic cancer radiotherapy. J Appl Clin Med Phys. 2023;24:e14123. https://doi.org/10.1002/acm2.14123

[36] Parikh PJ, Lee PP, Low DA, et al. A multi-institutional phase 2 trial of ablative 5-fraction stereotactic magnetic resonance-guided on-table adaptive radiation therapy for borderline resectable and locally advanced pancreatic cancer. Int J Radiat Oncol Biol Phys. 2023;117:799-808.

 DOI: 10.67692/IODT.26.7900

https://doi.org/10.1016/j.ijrobp.2023.05.033

[37] Chuong MD, Bryant JM, Herrera R, et al. Stereotactic MR-guided on-table adaptive radiation therapy (SMART) for borderline resectable and locally advanced pancreatic cancer: a multi-center, open-label phase 2 study. Radiother Oncol. 2024;191:110064. https://doi.org/10.1016/j.radonc.2023.110064

[38] Rudra S, Jiang N, Rosenberg SA, et al. Using adaptive magnetic resonance image-guided radiation therapy for treatment of inoperable pancreatic cancer. Cancer Med. 2019;8:2123-32. https://doi.org/10.1002/cam4.2100

[39] van Dams R, Wu TC, Kishan AU, et al. A multi-institutional experience of MR-guided liver stereotactic body radiation therapy. Adv Radiat Oncol. 2019;4:142-9. https://doi.org/10.1016/j.adro.2018.08.008

[40] Henke LE, Olsen JR, Contreras JA, et al. Phase I trial of stereotactic MR-guided online adaptive radiation therapy (SMART) for the treatment of oligometastatic or unresectable primary malignancies of the abdomen. Radiother Oncol. 2018;126:519-26. https://doi.org/10.1016/j.radonc.2017.11.032

[41] Hering A, Rischke HC, Henkenberens C, et al. MR-guided online adaptive stereotactic body radiotherapy of primary lung tumors and lung oligometastases. Strahlenther Onkol. 2024;200:878-87. https://doi.org/10.1007/s00066-024-02219-7

[42] Gelbart Pridan A, Meirovitz A, Cham S, et al. Outcome of the first 200 patients with prostate cancer treated with MRI-Linac at Assuta MC. Front Oncol. 2023;13:1137034. https://doi.org/10.3389/fonc.2023.1137034

[43] Grimbergen G, Hackett SL, van Ommen F, et al. Treatment planning for MR-guided SBRT of pancreatic tumors on a 1.5 T MR-Linac: a global consensus protocol. Clin Transl Radiat Oncol. 2024;49:100855. https://doi.org/10.1016/j.ctro.2024.100855

[44] Behzadipour T, Moftah W, Nazaryan V, et al. Failure mode and effects analysis for MR-guided adaptive radiotherapy. J Appl Clin Med Phys. 2024;25:e14207. https://doi.org/10.1002/acm2.14207

[45] Hehakaya C, van der Voort van Zyp JRN, Lagendijk JJW, et al. Health economic evaluation of the MRI-linac. Radiother Oncol. 2021;157:136-41. https://doi.org/10.1016/j.radonc.2021.01.011

[46] de Mol van Otterloo SR, Christodouleas JP, Blezer ELA, et al. The MOMENTUM study: an international registry for the evidence-based introduction of MR-guided adaptive therapy. Front Oncol. 2020;10:1328. https://doi.org/10.3389/fonc.2020.01328

[47] Keall PJ, Barber J, Bucci MK, et al. ICRU Report 97: MRI-guided radiation therapy using MRI-linear accelerators. J ICRU. 2022;22:1-100. https://doi.org/10.1177/14736691221082938